

Dileptons, Charm and Bottom in Relativistic Heavy-Ion Collisions

B. Kämpfer^a, O.P. Pavlenko^{a,b}, K. Gallmeister^a

^a*Forschungszentrum Rossendorf, PF 510119, 01314 Dresden, Germany*

^b*Institute for Theoretical Physics, 252143 Kiev - 143, Ukraine*

The relation of the thermal dilepton signal from deconfined matter, resulting in central ultra-relativistic heavy-ion collisions at RHIC and LHC energies, to the background yields from the Drell-Yan process and correlated semileptonic decays of open charm and bottom mesons is analyzed. We demonstrate that very stringent kinematical cuts offer a chance to identify the thermal signal in the continuum region.

1 Introduction

Since a long time the penetrating probes, such as dileptons and photons, are considered as nearly undisturbed messengers from hot and dense, strongly interacting matter produced in central ultra-relativistic heavy-ion collisions (cf. [1]). Indeed, in present SPS experiments ($\sqrt{s} = 15 \cdots 20$ GeV) the CERES collaboration reports a dilepton excess over the known hadronic cocktail in S + Au and Pb + Au collisions at invariant masses $M < 1$ GeV [2]. The order of magnitude of this excess can be attributed to a thermal source stemming mainly from pion annihilation, while the detailed shape of the spectrum is still matter of debate, e.g. it might reflect an in-medium changed ρ spectral function. Similarly, in the so-called intermediate mass region $M = M_\phi \cdots M_{J/\psi}$, as accessible in the acceptances of the HELIOS-3 and NA38/50 experimental set-ups, the conventional sources Drell-Yan (DY) and open charm decays seem also not to account for the observed data, i.e. there is also an excess [3]. It is just the intermediate mass region where all model calculations (cf. [1, 4]) predict best chances to see a thermal signal from deconfined matter.

For an illustration of that fact we display in Fig. 1 the time evolution of the thermal dilepton yield from purely deconfined matter for various invariant masses covering the intermediate mass region. Indeed, as seen in Fig. 1, the major amount (90%) of harder dileptons with $M = 4$ GeV stem from early ($\tau = 0.2 - 2$ fm/c) and hot ($T > 2T_c$) matter stages, while the more soft dileptons with $M = 1$ GeV are breded out mainly at temperatures around confinement temperature T_c and are strongly contaminated by dileptons from the hadron stage.

Analyzes of hadron particle ratios [5] and transverse momentum spectra [6] in present CERN-SPS experiments deliver temperatures of $T \sim \mathcal{O}(m_\pi)$. While this is a first step to pin down the production of a hot system in heavy-ion collisions, one is interested in signals which can identify much higher temperatures pointing to the necessary achievement of conditions for deconfinement, i.e. $T \gg \mathcal{O}(m_\pi)$. The measured hadron rapidity densities at SPS can be translated into maximum initial temperatures $T_i \sim \mathcal{O}(200)$ MeV when using Bjorken's estimate with a initial time $\tau_i = 1$ fm/c.

At higher beam energies one expects also much higher maximum temperatures achievable. On the same time, when going to higher center-of-mass energies \sqrt{s} , also the background from DY and the hadronic decay cocktail increases. In particular, correlated semileptonic decays of open charm and bottom constitute a severe background. In what follows we consider the beam energy dependence of the dilepton yield in the intermediate

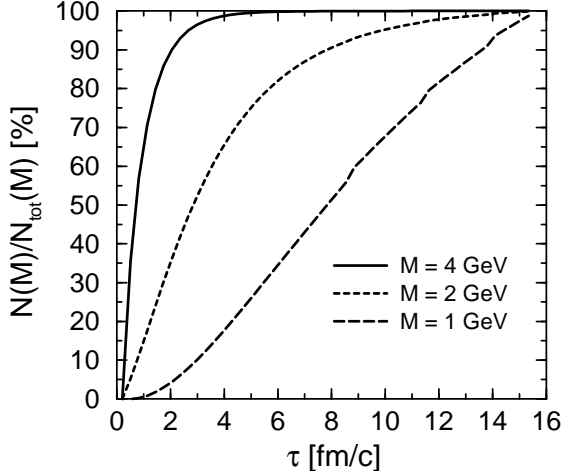


Figure 1: The time dependence of the normalized dilepton yield from purely deconfined matter at midrapidity for various invariant masses and for LHC initial conditions.

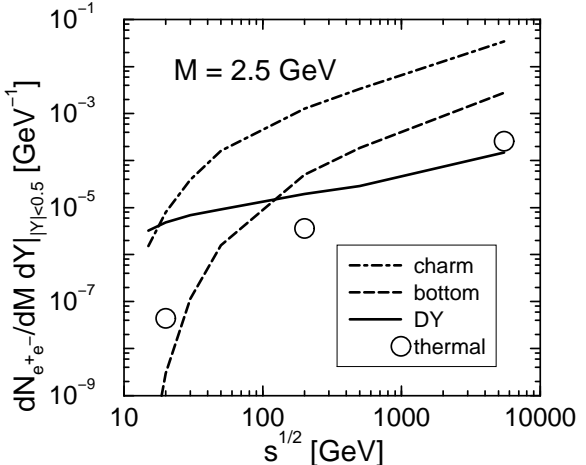


Figure 2: The dependence of dileptons from the lowest-order processes (DY and correlated semileptonic decays of open charm or bottom mesons) and the thermal source on $s^{1/2}$.

mass region (Section 2). It turns out that the mentioned background processes are much stronger than the thermal signal. We therefore study then in Section 3 various kinematical cuts, which suppress the background, and analyze the possibility to identify the thermal signal from deconfined matter. We focus here on this signal, since the dilepton radiation from hadron matter or a possible mixed phase will again deliver only a hint to relatively cold matter with $T \sim \mathcal{O}(m_\pi)$. Our conclusions can be found in Section 4.

2 Beam energy dependence

The necessary formulae for calculating the mentioned dilepton yields within a lowest-order approach are accumulated in [7, 8].

The initial conditions of the thermal era are estimated within a mini-jet picture. It allows to calculate the energy distribution and number distribution of mini-jets. Transport models and event generators point to the fact that this mini-jet plasma is thermalized at a very early time instant, $\tau_i \sim 0.2$ fm/c. The resulting values of initial temperatures T_i , gluon fugacities λ_i^g and resulting hadron rapidity densities dN_π/dy are listed in Tab. 1 [9]. The corresponding quark fugacities are usually $\lambda_i^q = \frac{1}{5} \lambda_i^g$.

	RHIC	LHC
T_i [GeV]	0.544	1.038
λ_i^g	0.41	0.25
dN_π/dy	1080	5204

Table 1: Estimates of initial values achievable at RHIC and LHC within the mini-jet picture. Nuclear shadowing effects are included.

With these propositions one gets the beam energy dependence of dileptons with $M \sim 2.5$ GeV at midrapidity as displayed in Fig. 2. The thermal source includes only purely deconfined matter. Note that at SPS energies the hadron and a possible mixed phase (both

ones not included here) represent also strong thermal sources. One observes that the ratio of DY dileptons to correlated open charm (bottom) decay dileptons drops down with increasing \sqrt{s} . Only in the region $\sqrt{s} < 20$ (120) GeV the Drell-Yan yield dominates above the charm (bottom) decay contribution. Note that the thermal yield estimates depend sensitively on the assumed initial parameters. In agreement with recent findings the thermal dilepton signal is up to two orders of magnitude below the correlated open charm decay dileptons in a wide range of invariant masses at LHC, RHIC [10] and SPS energies. Therefore, there is nowhere a preferred energy region; at high beam energies, however, one expects clearer deconfinement effects due to temperatures far above the confinement temperature.

The results displayed in Fig. 2 cover the full phase space. Any detector acceptance will suppress the various sources differently [7]. Energy loss of heavy quarks propagating through deconfined matter reduces also the open charm and bottom decay yields [11, 12]. Notice that with increasing invariant mass the thermal yield drops exponentially while, for instance, the Drell-Yan yields drops less, i.e. like a power law. Therefore, the results displayed in Fig. 2 can not be extrapolated in a simple manner to higher invariant masses.

3 Kinematical cuts

From all of these considerations the problem arises whether one can find such kinematical gates which enable one to discriminate the thermal signal against the large decay background. Since the kinematics of heavy meson production and decay differs from that of thermal dileptons, one can expect that special kinematical restrictions superimposed on the detector acceptance will be useful for finding a window for observing thermal dileptons in the intermediate mass continuum region. In particular, experimental cuts on the rapidity gap between the leptons can reduce considerably the charm decay background [10]. As demonstrated recently [7], the measurement of the double differential dilepton spectra as a function of the transverse pair momentum Q_\perp and transverse mass $M_\perp = \sqrt{M^2 + Q_\perp^2}$ within a narrow interval of M_\perp also offers the chance to observe thermal dileptons at LHC. In the present note we show that a large enough low- p_\perp cut on single electrons suppresses the mentioned background processes and opens a window for the thermal signal in the invariant mass distribution. We take into account the acceptance of the ALICE detector at LHC: the single electron pseudo-rapidity is limited to $|\eta_e| \leq 0.9$ and an overall low- p_\perp cut of 1 GeV is applied. We are going to study systematically the effect of enlarging the low- p_\perp cut on single electrons in the invariant-mass dilepton spectra at $\sqrt{s} = 5500$ GeV.

Since the energy of individual decay electrons or positrons has a maximum of about 0.88 (2.2) GeV in the rest frame of the decaying D (B) meson, one can expect to get a strong suppression of correlated decay lepton pairs by choosing a high enough low-momentum cut p_\perp^{\min} on the individual leptons in the mid-rapidity region. For thermal leptons stemming from deconfined matter there is no such upper energy limit and for high temperature the thermal yield will not suffer such a drastically suppression by the p_\perp^{\min} cut as the decay background. To quantify this effect we perform Monte Carlo calculations generating dileptons from the sources mentioned above. We first employ the transparent lowest-order calculations and then present more complete PYTHIA simulations.

As heavy quark masses we take $m_c = 1.5$ GeV and $m_b = 4.5$ GeV. We employ the HERA supported structure function set MRS D' [13] from the PDFLIB at CERN. Nuclear shadowing effects are not needed to be included for our present order of magnitude estimates.

The overlap function for central collisions is $T_{AA}(0) = A^2/(\pi R_A^2)$ with $R_A = 1.2A^{1/3}$

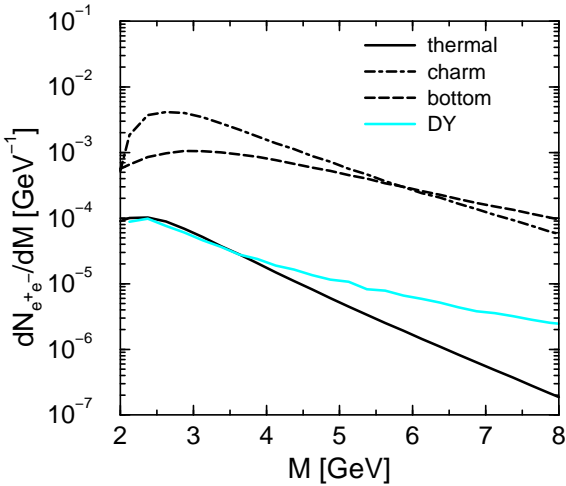


Figure 3: The invariant mass spectra of dileptons from the DY process, charm and bottom decays, and thermal emission. The single-electron low transverse momentum cut is $p_{\perp}^{\min} = 1$ GeV.

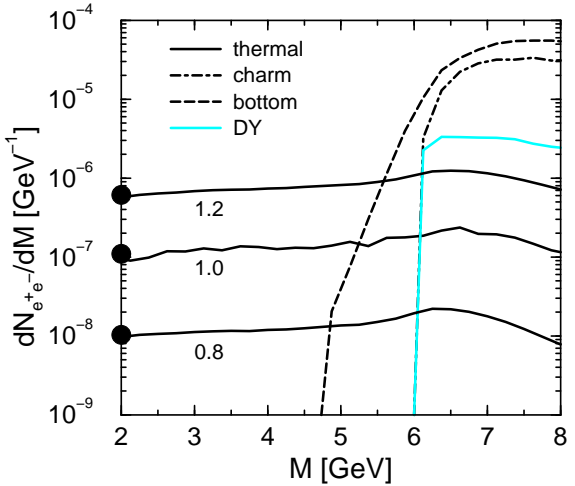


Figure 4: The same as in Fig. 3, but $p_{\perp}^{\min} = 3$ GeV. The fat dots indicate the estimates of the low- M thermal plateau as described in [8].

fm and $A = 200$. From a comparison with results of Ref. [10] we find the scale $\hat{Q}^2 = 4m_Q^2$ and $\mathcal{K}_Q = 2$ as most appropriate.

We employ a delta function fragmentation scheme for the heavy quark conversion into D and B mesons. Dilepton spectra from correlated semileptonic decays, i.e., $D(B)\bar{D}(\bar{B}) \rightarrow e^+Xe^-X$, are obtained from a Monte Carlo code which utilizes the inclusive primary electron energy distribution as delivered by the JETSET part of PYTHIA 6.1. The heavy mesons are randomly decayed in their rest system and the resulting electrons then boosted appropriately. The average branching ratio of $D(B) \rightarrow e^+X$ is taken as 12 (10)%.

The results of our lowest-order calculations of the invariant mass spectrum for various values of p_{\perp}^{\min} are displayed in Figs. 3 and 4 for LHC energies. One observes that the thermal dilepton signal with a single-electron low-momentum cut-off $p_{\perp}^{\min} = 3$ GeV exhibits an approximate plateau in the invariant mass region $2 \text{ GeV} \leq M \leq 2p_{\perp}^{\min}$. The physical information encoded in the continuum spectrum is discussed in [14]. The main point is that the cut $p_{\perp}^{\min} = 3$ GeV causes a strong suppression of the correlated charm decay and DY background in the region $M \leq 2p_{\perp}^{\min}$. The above value of the invariant mass threshold can be estimated by using the relation $M^2 = 2p_{\perp+}p_{\perp-}[\text{ch}(y_+ - y_-) - \cos(\phi_+ - \phi_-)]$, where ϕ_{\pm} denote the azimuthal angles of the leptons in the transverse plane. In order to exceed the cut p_{\perp}^{\min} most easily, the decay leptons should go parallel to the parent heavy mesons, which in turn are back-to-back (in the transverse plane) in lowest order processes. As a consequence, $\cos(\phi_1 - \phi_2) \approx -1$ and the minimum invariant mass becomes $M^{\min} \approx 2p_{\perp}^{\min}$ for such decay pairs. For correlated bottom decay the electron energy is larger in the meson rest system and both leptons can more easily overcome the threshold p_{\perp}^{\min} without such strong back-to-back correlation. Selecting, however, electrons with $p_{\perp} > p_{\perp}^{\min} = 3$ GeV one can also get the corresponding threshold like behavior for the lepton pairs from correlated bottom decay as seen in Fig. 4. Therefore the thermal signal becomes clearly visible for such a value of p_{\perp}^{\min} due to the strong suppression of the considered background channels.

The threshold behavior does not change if we include in our calculations energy loss effects of heavy quarks in deconfined matter. Such effects cause mainly a suppression of the

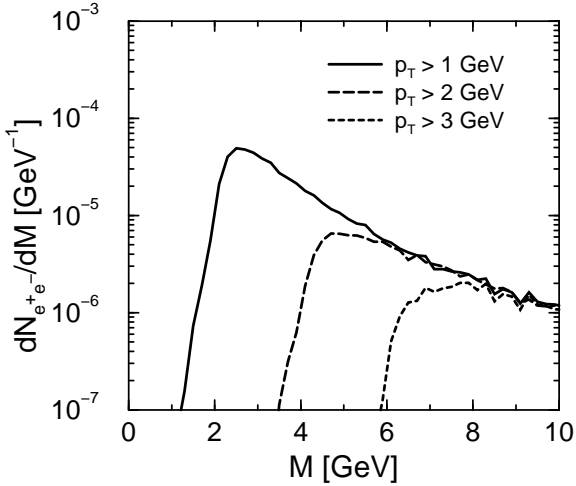


Figure 5: The invariant mass spectra of dileptons from the DY process for $p_{\perp}^{\min} = 1, 2$ and 3 GeV (from left to right). The curves depict results of PYTHIA with default switches.

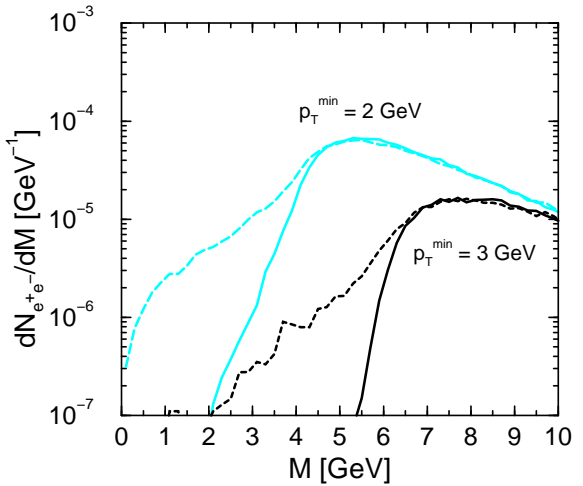


Figure 6: The invariant mass spectra of dileptons from correlated open bottom meson decays for $p_{\perp}^{\min} = 2$ and 3 GeV as delivered by PYTHIA (dashed curves: default switches, solid curves: without initial state radiation).

decay contributions (cf. [11, 12]). We also mention that shadowing effects, not included in our Drell-Yan and heavy quark production estimates, will diminish these yields somewhat.

The lowest order DY yield has anyway $M^{\min} = 2p_{\perp}^{\min}$. From the above given relations for M and M_{\perp} one can derive the inequality $M \geq 2p_{\perp}^{\min} \sqrt{1 - \left(\frac{Q_{\perp}}{2p_{\perp}^{\min}}\right)^2}$. This relation tells us that in the region $M < 5$ (4) GeV only pairs with total transverse momentum $Q_{\perp} > 3.25$ (4.5) GeV can contribute if $p_{\perp}^{\min} = 3$ GeV. Since the next-to-leading order DY distribution $dN/dM^2 dQ_{\perp}^2 dY$ drops from $Q_{\perp} \approx 0$ to 3 - 4 GeV by nearly three orders of magnitude [15] one can estimate a small higher order DY contribution in the small- M region. To quantify the smearing of the threshold effect by an intrinsic p_{\perp} distribution of initial partons we perform simulations with the event generator PYTHIA (version 6.104 [16]) with default switches. Results are displayed in Fig. 5 and show that the sharp threshold effect from the above lowest-order Drell-Yan process is indeed somewhat smeared out, however, the small- M region is still clean. It turns out that the initial state radiation of partons before suffering a hard collision is the main reason for rising the pair Q_{\perp} and for smearing out the sharp threshold effect, while the intrinsic p_{\perp} distribution of partons causes minor effects.

Let us now consider heavy quark pairs. Here, the intrinsic p_{\perp} distribution, and both initial and final state radiations of the partons can cause a finite Q_{\perp} and thus destroy the strong back-to-back correlation, i.e. $p_{\perp 1} \neq p_{\perp 2}$. In Fig. 6 we show results of simulations with PYTHIA for the bottom channel, where the resulting primary dileptons from all correlated open bottom mesons are displayed. One observes that the initial state radiation causes a pronounced smearing of the threshold effect discussed above. Without the initial state radiation, as implemented in PYTHIA, the threshold effect is recovered. The intrinsic p_{\perp} distribution and final state radiation are negligible. The conclusion of such studies is that an enlarged value of p_{\perp}^{\min} is necessary to keep clean the low- M region from open bottom decay products. For charm the smearing effect due to initial state radiation in PYTHIA is

efficiently suppressed by the large enough low- p_\perp cut of $p_\perp^{\min} = 3$ GeV. The different behavior of charm and bottom stem from the fact that the bottom- p_\perp distribution is much wider. As a consequence, the bottom is evolved in the average to much larger values of the resolution scale \hat{Q}^2 thus experiencing stronger kicks by initial state radiation. In agreement with our previous findings [12], bottom therefore causes the most severe background processes at LHC energies.

With PYTHIA also the dileptons from single decay chains of open bottom, like $B^0 \rightarrow e^+ D^- (\rightarrow e^- \bar{X}) X$ or $B^0 \rightarrow e^+ D_{2010}^* (\rightarrow \bar{D}^0, [\rightarrow e^- X'] \bar{X}) X$, are accessible. These channels provides a contribution peaking at 1.5 GeV; the cut $p_\perp^{\min} = 3$ GeV pushes all invariant masses below 3 GeV. Therefore, unless enlarging p_\perp^{\min} considerably, it will be difficult to suppress kinematically the background below the thermal signal at invariant masses $M < 3$ GeV. Probably explicit identification and subtraction of the bottom contribution is needed in this region.

Indeed, as recently found by the ALICE-GSI group [18], via exact tracking and vertex reconstruction one can suppress a substantial part of the open charm and bottom decay electrons in the midrapidity region. Therefore, the need of stringent cuts is relaxed somewhat and realistic count rates are to be expected.

In this respect we would also like to point out that an explicit measurement of the inclusive single-electron p_\perp -spectra from open charm and bottom decays contains valuable information [7]. Namely the energy losses due to induced gluon radiation [17] of heavy quarks propagating through deconfined matter change the resulting momentum distribution of the open charm and bottom mesons and, as a consequence, the decay electrons exhibit a significantly changed p_\perp spectrum (for details consult [7]). Since such an effect does not appear in pp collisions, the verification of a modified electron spectrum from identified charm and bottom decays would offer a hint to the creation of deconfined matter. The studies in [18] demonstrate that tracking cuts offer the chance to get a "signal"-to-background ratio of 98%, where "signal" means here the decay electrons from charm and bottom. Therefore, such a measurement seems to be feasible with ALICE at LHC. To illustrate the order of magnitude of the expected effect we show in Fig. 7 the transverse momentum spectrum of decay electrons from open charm and bottom mesons in a lowest-order calculation as described above [7]. One can fit the distribution by $dN_e/dp_\perp \propto \exp(-p_\perp/T_e)$ in the interval $2.5 \text{ GeV} < p_\perp < 4.5 \text{ GeV}$ and finds a change of the slope parameter T_e from 850 MeV (without energy loss) to 640 MeV (with energy loss).

4 Summary

In summary we analyze the beam energy dependence of various expected sources of dileptons in ultra-relativistic heavy-ion collisions. Already at $\sqrt{s} > 20$ GeV a copious production of charm gives rise to a dominant contribution to the dilepton spectrum at intermediate invariant masses. Taking into account the ALICE detector acceptance we study systematically the effect of single-electron transverse momentum cuts. We find a threshold like behavior of the invariant mass spectra of dileptons from primary correlated charm and bottom decays and Drell-Yan yield as well: these sources are suppressed at $M < M^{\min} \approx 2p_\perp^{\min}$ for $p_\perp^{\min} > 3$ GeV. In contrast to this, the thermal dilepton signal exhibits a plateau in this region which offers the opportunity to identify them and to gain information on the initial stages of deconfined matter at LHC energies. The same mechanism also works at RHIC energies, however the expected count rates are too small to make such a strategy feasible. The complex decay chains of heavy mesons, in particular open bottom, and the resulting

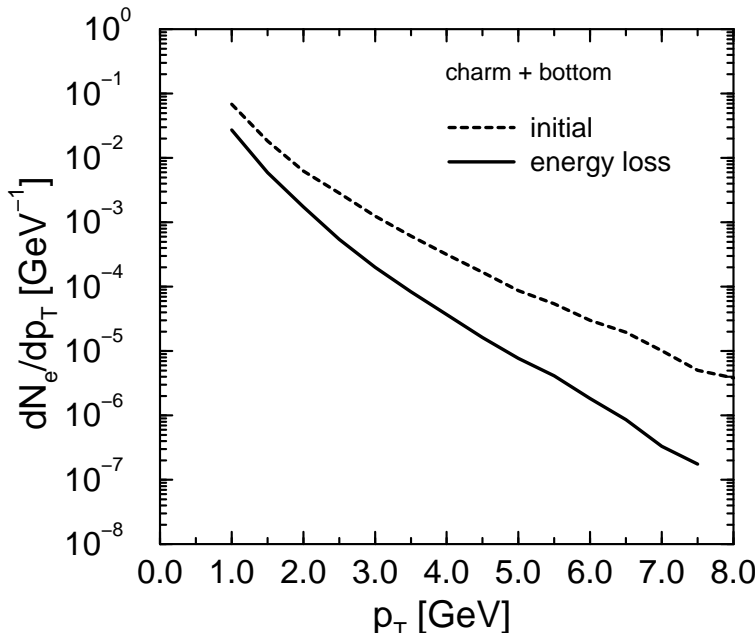


Figure 7: The transverse momentum spectra of single electrons from D and B meson decays at RHIC energy. Displayed are the spectra without ("initial") and with energy loss according to model II in [7].

combinatorial background make an explicit identification of the "hadronic cocktail" very desirable to allow a safe identification of the thermal signal from deconfined matter.

The selection of decay electrons from open charm and bottom can signalize the presence of deconfined matter via a modified single-electron p_{\perp} spectrum in comparison with pp collisions.

Stimulating discussions with P. Braun-Munzinger, Z. Lin, R. Vogt, G. Zinovjev are gratefully acknowledged. O.P.P. thanks for the warm hospitality of the nuclear theory group in the Research Center Rossendorf. The work is supported by BMBF grant 06DR829/1 and WTZ UKR-008-98.

References

- [1] P.V. Ruuskanen, in *Quark-Gluon Plasma*, edited by R. Hwa, (World Scientific, Singapore 1990), p. 519.
- [2] I. Ravinovich et al. (CERES), Nucl. Phys. A **638**, 123 (1998)
- [3] A.L.S. Angelis et al. (HELIOS/3), CERN-EP/98-82
E. Scomparin et al. (NA38/50), www.cern.ch/NA50/papers.html
- [4] B. Kämpfer, O.P. Pavlenko, A. Peshier, G. Soff, Phys. Rev. C **52**, 2704 (1995)
- [5] P. Braun-Munzinger, J. Stachel, J.P. Wessels, N. Xu, Phys. Lett. B **365**, 1 (1996)
- [6] B. Kämpfer, hep-ph/9612336;
B. Kämpfer, O.P. Pavlenko, A. Peshier, M. Hentschel, G. Soff, J. Phys. G **23**, 2001 (1997)

- [7] K. Gallmeister, B. Kämpfer, O.P. Pavlenko, Phys. Rev. C **57**, 3276 (1998)
- [8] K. Gallmeister, B. Kämpfer, O.P. Pavlenko, FZR-235 (1998)
- [9] B. Kämpfer, O.P. Pavlenko, Phys. Lett. B **391**, 185 (1997)
- [10] S. Gavin, P.L. McGaughey, P.V. Ruuskanen, R. Vogt, preprint LBL-37981, Phys. Rev. C **54**, 2606 (1996)
- [11] E.V. Shuryak, Phys. Rev. C **55**, 961 (1997)
Z. Lin, R. Vogt, X.-N. Wang, Phys. Rev. C **57**, 899 (1998)
- [12] B. Kämpfer, O.P. Pavlenko, K. Gallmeister, Phys. Lett. B **419**, 412 (1998)
- [13] A.D. Martins, W.J. Stirling, R.G. Roberts, Phys. Lett. B **306**, 145 (1993)
- [14] K. Gallmeister, B. Kämpfer, O.P. Pavlenko, contribution in this volume
- [15] S. Gavin, S. Gupta, R. Kauffman, P.V. Ruuskanen, D.K. Srivastava, R.L. Thews, Int. J. Mod. Phys. A **10**, 2961 (1995)
- [16] T. Sjöstrand, Comp. Phys. Commun. **82**, 74 (1994),
cf. also <http://hep.lu.se/tf2/staff/torbjorn/Pythia.html>
- [17] R. Baier et al., Phys. Lett. B **345**, 277 (1995), Nucl. Phys. B **483**, 291 (1997), Nucl. Phys. B **484**, 265 (1997), hep-ph/9803473
- [18] P. Braun-Munzinger, contribution in this volume;
cf. also <http://www.gsi.de/~alice/transp/philippe/tr14.ps>

